Designing Next Generation of Photon Upconversion: Recent advances in Organic Triplet-triplet Annihilation Upconversion Nanoparticles

Ling Huang[a], **Eugenia Kakadiaris**[a], **Tereza Vaneckova**[a,b], **Kai Huang**[a], **Marketa Vaculovicova**[b], and **Gang Han**[a]

[a]Department of Biochemistry and Molecular Pharmacology, University of Massachusetts Medical School, Worcester, Massachusetts 01605, United States.

[b]Department of Chemistry and Biochemistry Mendel University in Brno, Brno, 61300, Czech Republic

Abstract

Organic triplet-triplet annihilation upconversion (TTA-UC) nanoparticles have emerged as exciting therapeutic agents and imaging probes in recent years due to their unique chemical and optical properties such as outstanding biocompatibility and low power excitation density. In this review, we focus on the latest breakthroughs in such new version of upconversion nanoparticle, including their design, preparation, and applications. First, we will discuss the key principles and design concept of these organic-based photon upconversion in regard to the methods of selection of the related triplet TTA dye pairs (photosensitizer and emitter). Then, we will discuss the recent approaches s to construct TTA-UCNPs including silica TTA-UCNPs, lipid-coated TTA-UCNPs, polymer encapsulated TTA-UCNPs, nano-droplet TTA-UCNPs and metal-organic frameworks (MOFs) constructed TTA-UCNPs. In addition, the applications of TTA-UCNPs will be discussed. Finally, we will discuss the challenges posed by current TTA-UCNP development.

Keywords

Introduction:

Photon-upconverting (UC) convert low-energy photons into high-energy ones.[1–2] In past decades, lanthanide ions-doped inorganic nanoparticles were widely applied in photodynamic therapy, photoactivated drug release, fluorescence sensors, and optogenetic techniques.[3–6] However, this type of upconversion nanoparticles have certain drawbacks

Corresponding: Gang.Han@umassmed.edu.

such as the requirement of the laser light with relatively high excitation power density and inherently suboptimal upconversion quantum yield. In addition, the toxicity of lanthanide ions in the organism needs further exploration.[7–8] Seeking to improve upon these inorganic lanthanide nanoparticles, scientists have begun to explore organic TTA-UC due to their special optical properties such as low excitation power density, intense absorption of excitation light, high upconversion quantum yield, and readily tunable excitation/emission wavelength.[9–14] In TTA-UC, as shown in Scheme 1a, the photosensitizer absorbs low energy photons and transits to single state (S_1) and subsequently to the triplet excited state (T_1) by in intersystem crossing process (ISC) of photosensitizer, and then the triplet-triplet energy transfer (TTET) generates from photosensitizer to emitter. Finally, the triplet states of emitter annihilation (TTA) produce high energy upconverted photons. [9–14]

In order to achieve versatile applications of TTA-UC in cancer therapy, fluorescence sensors and drug delivery, researches have attempted to explore the methods to develop of highly effective TTA-UCNPs. [2, 14] However, these endeavors encountered a series of challenges: (1) molecular oxygen can easily quench the triplet state of photosensitizers and emitters; (2) the aggregation of photosensitizers and emitters can have detrimental influences on the optical properties in the TTA-UCNPs; (3) the mobility of photosensitizers and emitters in TTA-UCNPs limits the triplet-triplet energy migration (TTET and TTA process) and concomitants upconversion efficiency. In this review, we will start by discussing how to design efficient TTA-UC dye pairs including the basic theory and principles. In the second section, recent advances in the preparation of TTA-UCNPs including silica TTA-UCNPs, lipid-coated TTA-UCNPs, polymer-encapsulated TTA-UCNPs, nano-droplet based TTA-UCNPs and metal-organic frameworks (MOFs) constructed TTA-UCNPs will be presented (scheme 1b). In addition, we will show the multiple applications of TTA-UCNPs in bio-imaging, photo-targeting, and tumor treatment. Finally, we will suggest possible future directions and application areas of TTA-UCNPs.

1 The basic theory and principles of TTA-UC.

In general, the TTA-UC process is an anti-Stokes shift delay process. The TTA-UC emission spectrum presented the similarity to the fluorescence spectrum of the emitter, but the upconversion emission presents a longer delay in the lifetime (microseconds) than the original fluorescence lifetime of the emitters (nanoseconds). The upconversion intensity presents a quadratic ($x2$) dependence on the incident light power under low excitation power density because two triplet states of emitters are required in the TTA process. After the transition threshold (I_{th}), TTA-UC presents a linear dependence under high power density excitation irradiation since the emitters are saturated [9–14].

In the TTA-UC processes, the intense light absorption of photosensitize is beneficial for harvesting more photons. In addition, the efficient ISC process is critical to the triplet quantum yield of the photosensitizer. Moreover, the long triplet excited lifetime of the photosensitizer is required for triplet-triplet energy transfer from the photosensitizer to the emitter. For the emitters, they should have a lower triple excited state than that of the photosensitizer in order for the TTET process to occur. The high fluorescence quantum yield is important in improving the upconversion efficiency. In addition, the emitter of double

triplet energy ($2T_1$) should be greater than the singlet energy (S_1) of the emitter which is essential to the TTA process. [9–14]

In recent years, a series of TTA photosensitizers that contain organic photosensitizers and noble metal complexes (Ru (II), Pt (II), Ir (III) and Re (I)) were reported. [17–20] In this review, we will focus on these generally used and commercially available photosensitizers such as green-absorbing platinum/palladium octaethylporphyrin (PtOEP/PdOEP),[21] red-absorbing meso-tetraphenyl-tetrabenzoporphine platinum/palladium (PtTPBP/PdTPBP), [22] and near infrared absorbing palladium(II) octabutoxyphthalocyanine ($PdPc(OBu)_8$) as well as metal-free BODIPY based photosensitizers. [23] In particular, PtOEP has intense absorption in visible green region, long triplet state lifetime (90 μs) and triplet excited state energy level (1.92 eV). For example, when combined with the emitter of 9, 10-diphenyl anthracene (DPA), TTA-UC quantum yield was observed to be excellent. [24–26] Compared to PtOEP, the absorption wavelength of PdTPBP is red-shifted to red (635 nm). PdTPBP is suitable for TTA-UC due to robust photostability, long triplet excited lifetime (223.7 μs) and adjusted triplet excited state energy level (1.56 eV). When combined with perylene, BDP-515, and BDP-546, the bright upconversion from red to blue /green/orange was reported. [27] NIR absorbing TTA-UC is advantageous in biological applications such as deep tissue penetration and weak photo-damage for the organism. [28–29] $PdPc (OBu)_8$ was proposed to use due to its intense absorbance in NIR region. When combined with a rubene emitter, NIR to visible light upconversion was able to be detected. [25] In addition, metal free BODIPY based photosensitizers were recently developed. BODIPY photosensitizers have shown attractive photophysical properties such as strong absorbance, high triplet state quantum yield, and long triplet excited lifetime. More importantly, the flexible molecular structure provides a platform to prepare and screen the best TTA-UC systems. [30–32]

2.   The strategy of preparation of TTA-UCNPs

TTA-UC has a larger absorbing cross-section area than rare earth-doped upconversion nanoparticles, high upconversion quantum yield under low excitation power density.[2,5] However, preparation of highly efficient TTA-UCNPs remains challenging due to the molecular oxygen quenching and chromophore aggregation in nanoparticles. Along with nanotechnology development, many preparation strategies were reported in past decades. In this section, we will discuss and summarize the preparations of TTA-UCNPs. [9–14]

2.1.   Liposome-encapsulated TTA-UCNPs—Liposome-encapsulated nanomaterials have been widespread in the biological and clinical studies. Amphiphilic phospholipids especially have seen particular success and have been approved to use in the clinic by the United States Food & Drug Administration (FDA). [33–35] Therefore, liposomes were one of the first material considered to prepare the TTA-UCNPs.

For example, Askes *et al.* selected liposomes to prepare red or green light to blue TTA-UCNPs. As shown in Figure 2, the blue up-converting liposomes can trigger the photo-dissociation of Ru-2 from PEGylated liposomes using a red laser source (630 nm). In the TTA-UC liposomes, PdTPBP is the red absorbing photosensitizer and perylene is the emitter. Due to the triplet excited state energy level of perylene matching well with PdTPBP,

the PdTPBP/perylene system presents high red to blue upconversion quantum yield. The hydrophobic moieties of lipid can alleviate the aggregation of PdTPBP and perylene and the mobility of PdTPBP and perylene. Using the TTA-UC liposomes, the photo-activated Ru complexes system was constructed by the sulfur coordination Ru complexes. Upon excited by the red laser (630 nm), the bright blue upconversion was re-absorbed by Ru complexes (Ru-2), leading to the water coordination Ru complexes (Ru-1) releasing from the TTA-UC liposomes. [36]

In addition, compared to conventional fluorescence agents such as typical dyes and semiconductor quantum dots, due to the advantages of anti-Stokes fluorescence reducing the background auto-fluorescence and eliminating the potential damage of the living tissue, TTA-UCNPs presented high signal-noise ratio in the cell imaging with lower power excitation irradiation. [37–39] To this end, as shown in Figure 3, Mattiello *et al.* provided a facile protocol to prepare the TTA-UC nanomicelles which contain PtOEP as photosensitizer and DPA as the emitter. The photosensitizer of PtOEP not only has intense absorption in the green region but also has long triplet lifetime and robust photostability. The emitter of DPA has high fluorescence quantum yield (> 90 %) and suitable triplet excited energy level with PtOEP (1.72 eV). The dual dyes were coated by the commercially available surfactant −Kolliphor EL. Due to the highly efficient TTET process from PtOEP to DPA, the red phosphorescence of PtOEP was dramatically quenched in TTA-UC nanomicelles. The result demonstrated that surfactant Kolliphor EL is an excellent matrix to reduce the dyes aggregation and keep mobility of PtOEP and DPA in TTA-UC nanomicelles. More important, the upconversion quantum yield of TTA-UC nanomicelle is up to 6.5 % under 0.1 W/cm^{-2} in the water in the air. Due to the low toxicity of TTA-UC nanomicelles, these nanomicelles were used for anti-Stokes fluorescence imaging of 3T3 cells under low power excitation intensity. [40] The TTA-UC nanomicelles presented dual color cell imaging, the red emission from the phosphorescence of PtOEP and the blue emission from the upconversion process. This dual color feature of TTA-UC nanomicelle is useful to construct the ratio-metric upconversion imaging so as to improve the signal-noise ratio.

Moreover, as shown in Figure 4, Kouno *et al.* synthesized the amide bond and quaternary ammonium salt modified DPA derivative (A-1). In this molecule, the hydrophobic DPA moiety orderly self-assembled by π-π stacking interactions and the hydrogen bond from the amide further stabilized the supramolecular structure. The cation not only enhanced the water-soluble of DPA liposome but also improved the binding affinity with the photosensitizer of Pt porphyrin by ion-ion interaction. The photosensitizers and emitters self-assembly not only improved the triplet-triplet energy migration due to the reducing of the intermolecular distance, but also minimized the molecular oxygen quenching in water. More importantly, high upconversion quantum yield (7%) was observed in the water and in the presence of oxygen. [41–42]

2.2. Silica-coated TTA-UCNPs—Silica nanoparticles (silica NPs) have been FDA approved for biological applications because of their versatile surface chemistry, outstanding *in vitro* and *in vivo* biocompatibility, rich nanopores, and large surface area. [43] Silica NPs offer numerous advantages. For example, silica NPs present well defined and tunable structures in the size, morphology, and porosity. In addition, silica NPs can be easily

synthesized from inexpensive starting materials. Moreover, silica NPs can befunctionalized by well-established siloxane chemistry. Meanwhile, the internalization into the nanostructure of silica can increase the chemical stability of loaded species. Moreover, silica NPs exhibit excellent transparence in the ultraviolet, visible and NIR region. [43–48] Benefited from these properties, silica NPs are used as the hosts for the preparation of TTA-UCNPs. In this section, we will discuss the silica-coated TTA-UCNPs design, preparation, and application *in vivo* small animal imaging.

In this regard, Li and co-workers reported TTA-UCNPs by silica-coated TTA-UCNPs containing PdOEP and DPA. Firstly, the PdOEP and DPA were encapsulated by the amphiphilic polymer (Pluronic® F-127). The hydrophobic moiety can avoid the PdOEP and DPA aggregations in nanoparticles and the hydrophilic moiety enhances the water-soluble of TTA-UCNPs. Then the silica shell coated polymer can stablize the TTA-UCNPs and decrease the molecular oxygen quenching of the triplet state of PdOEP. The silica-coated TTA-UCNPs not only have a uniform and narrow size distribution, but also presents high upconversion quantum yield (4.5%) in the aqueous solution in the air. In addition, the nanoparticles presented excellent photostability. Due to the low cytotoxicity of the silica-based TTA-UCNPs for cells, the nanoparticles showed a high signal-noise ratio in the living cell imaging. In the small animal imaging, the silica-based TTA-UCNPs can completely eliminate the mice auto-fluorescence, so that the silica-coated TTA-UCNPs presented excellent signal-to-noise ratio with low power laser irradiation (532 nm, 8.5 mW/cm^2) in lymph node imaging of living mouse. This study not only provides a protocol to synthesize the bright silica TTA-UCNPs but also it opens new perspectives for TT-UCNPs in bioimaging *in vivo*. [49]

Moreover, small animal imaging can precisely obtain anatomical and physiological details of living systems. This superiority is beneficial in realizing tumor malignancy in the early stage. The development of the early tumor diagnosis is significant to treat cancer. To do so, Kwon and co-workers reported that the self-assembly nano-emulsion coated by silica. [50] In this silica coated TTA-UCNPs, the core of unsaturated alkyl chain of oleic acid not only kept the mobility of PdTPBP and emitters but also reduced the molecular oxygen quenching triplet state of PdTPBP. In addition, the anion of carboxylic acid self-assembled with an amine compound to change the zeta potential of oleic acid encapsulated nanomicelles. At last, the silica shell grew on the nanomicelles to stable the TTA-UC nanomicelles. Additionally, the silica shell has many sites for further surface modification, that allow conjugation with targeted molecules, such as specific tumor-targeted peptides and antibodies. The silica-coated TTA-UCNPs not only can uniformly disperse in water but also presented high upconversion quantum from red to blue light in saturated water. Using this method, the dual color silica-based TTA-UCNPs were prepared. In these TTA-UCNPs, red-absorbing PdTPBP is the photosensitizer. When combined with perylene, the red to blue silica TTA-UCNPs were obtained. 9, 10-bis (phenylethynyl) anthracene is emitter due to the high fluorescence quantum yield and matched triplet state energy level with PdTPBP, the TTA-UCNPs presented green emission upon the red light irradiation. The dual color TTA-UCNPs were conjugated with two types of peptides to selectively target breast or colon cancer cells, respectively. The dual color emission silica coated TTA-UCNPs can efficiently

accumulates in the breast and colon tumor by enhanced permeability and retention effect (EPR). [51]

2.3. Polymer encapsulated TTA-UCNPs

Polymeric nanoparticles have recently attracted increasing attention in the biological applications due to their attractive optical properties, easy preparation, and robust photostability in bio-imaging. Additionally, polymer nanoparticles possess other advantages, for example, tunable excitation/emission wavelength, good biocompatibility, potential biodegradability, and facile surface functionalization. [52–57] Owing to these benefits, the TTA-UC based polymer encapsulated nanoparticles were developed.

In general, polymer encapsulated TTA-UCNPs were divided into two types depending on the preparation methods. The first type of polymer encapsulated TTA-UCNPs were synthesized by "bottom-up" strategy. [58–62] As shown in figure 7, the monomer, photo-initiator, solvent, photosensitizer, and emitter were mixedin glass capillary microfluidic device. The monomer was polymerized to encapsulate the photosensitizer, emitter and solvent. The multicolor TTA-UCNPs can be easily prepared by tuning the photosensitizers and emitter. In order to avoid the molecular oxygen-induced upconversion quenching and to reduce the chromophore aggregation-induced upconversion quenching, polymer encapsulated TTA-UCNPs with ultrathin double shells were developed by a microfluidic flow-focusing device. The encapsulation efficiency of TTA-UCNPs can be controlled by tuning the flow rates and surface affinity with geometric confinement. In these polymer encapsulated TTA-UCNPs, The hydrocarbon oil core provides an ideal matrix to favor the TTET and TTA process. The resin outer phase was formed by photo-curation to stabilize the TTA-UCNPs. Moreover, the containing heavy-atom compound -doped core is beneficial to improve the TTA upconversion quantum yield [61]. Although the "bottom-up" strategy can achieve high quantum yield and multicolor TTA-UCNPs, the size of particles is large (up to a few microns). The big sized particle is not ideal for applications in biology. In addition, preparation of these types of TTA-UCNPs needs a complex microfluidic flow-focusing device, which limits their feasibility.

Other polymer encapsulated TTA-UCNPs were prepared by amphiphilic polymers directly coating the photosensitizers and emitters. [63–66] In these TTA-UCNPs, the hydrophobic dyes were encapsulated by a hydrophobic moiety of polymer. The hydrophilic moiety can efficiently disperse the TTA-UCNPs in water. Under low energy photons irradiation, the TTA-UCNPs can generate the high energy photons. Compared to the liposomes coated TTA-UCNPs, the polymer-based TTA-UCNPs presented rigidity, fluidity, plasticity, permeability and facile surface modifications. As shown in Figure 8, Askes and co-workers chose the copolymer to coat the PdTPBP and perylene. In this copolymer, the hydrophobic moiety is PIB, which can avoid molecular oxygen quench triplet state of photosensitizers. Additionally, PIB also presents high chemical stability and low toxicity for the organism. The hydrophilic moiety is PEG which is a biocompatible and easily functionalized polymer. The stability of red-to-blue TTA-UCNPs was prepared by PIB-PEG co-polymer coated. Due to the antioxidants reducing the oxygen quenching, the TTA-UC intensity obviously enhanced. Moreover, the PIB-PGE encapsulated TTA-UCNPs were used for cell imaging.

Thought co-incubation with an antioxidant cocktail, the TTA-UC intensity enhanced over one order of magnitude. [64]

Such polymer encapsulated TTA-UCNPs are also used to control cell adhesion by photoactivation peptides. Wang and co-workers prepared a photo-activation functionalized amphiphilic polymer–polylactic acid (PLA)-polyethylene glycol (PEG)-cyclo-(RGDfK)-DEACM (PLA-PEG-cyclo-(RGDfK) -DEACM). In this polymer, the hydrophobic core contains the PtOEP, DPA and the DEACM protection cyclo-(RGDfK) peptide. When stimulated by green light LED, the blue photons were then transferred to a hydrophobic photo-cleavable group (DEACM) by FRET mechanism. After the cleavage of DEACM, the hydrophilic peptide was allowed to move to the surface from the core of NPs. Finally, cell uptake ability of TTA-UCNPs was improved due to the fact that specific binding with the receptor of cells. Using these TTA-UCNPs mediated photocleavage system, Liu and co-workers presented *in vivo* TTA-UCNPs photo-targeting in a living mice tumor model. Under low power excitation density, the TTA-UCNPs were effectively activated during a short time. In this process, the TTA-UCNPs did not cause tissue injury. More importantly, the photo-targeted strategy can improve the TTA-UCNPs accumulation in the tumor site but not in the liver and spleen. The new targeted methods can efficiently avoid the off targeting for TTA-UCNPs. [65–66] This study not only further enhances the application of TTA-UCNPs in biomedicine, but also paves the way for a new photoactivation strategy for targeting molecules releasing *in vitro* and *in vivo* under low power light irradiation. However, in this TTA-UCNPs-mediated photocleavage system, the green light did not have deeper tissue penetration ability than red light and NIR.

2.4. Nanodroplet based TTA-UCNPs—Dye aggregation and molecular oxygen quenching seriously decrease the TTA-UC intensity in nanoparticles. To obtain the bright TTA-UCNPs, it is very important to develop a new strategy to reduce the dyes aggregation and to avoid the oxygen quenching triplet state of photosensitizers. [9–14] In order to address these drawbacks, Li and co-workers developed a general strategy to prepare the TTA-UCNPs. [67] As shown in Figure 10, the soybean oil is found to be able to maintain the mobility of photosensitizers and emitters. In this design, molecular oxygen produces singlet oxygen by photosensitizer with light irradiation, and then singlet oxygen can react and be exhausted with an unsaturated bond as to eliminate the molecular oxygen. In order to let soybean oil disperse in water, BSA-Dextran was used to coat the soybean oil nanodroplet. In these TTA-UCNPs, BODIPY-based emitters were used due to their high fluorescence quantum yield, robust photostability and matched triplet excited state energy level with PdTPBP. In addition, BODIPY emitters are easily tuned the emission color by modified the molecular structure. According to these advantages of BODIPY, BDP-515 and BDP-546 were used emitters. The TTA-UC nanodroplet not only has high upconversion quantum yield but also is easy to prepare by tuning the photosensitizers and emitters. Due to the low cytotoxicity of TTA-UC nanodroplet, the biocompatible nanomaterials were successfully used to create multicolor lymph node imaging *in vivo* of living mice and high signal-to-noise ratios were observed with low power excitation irradiation. [67]

Such nanodroplet based TTA-UCNPs were also recently used as new phototransducers to photo-activates the prodrug to treat cancer. [71] Usually, the light sensitive prodrug is made

by conjugating the drug molecules with photomasks such as coumarin, o-nitrobenzene. [68–70] However, the absorption of this photomask is located in ultraviolet (UV) region (< 400 nm) which is limited to develop the photoactivation small molecules releasing in deep tissue level. As shown in Figure 11, we developed a new TTA-UCNPs based photocleavage system. The silica nanopores provide much space to stabilize the nanodroplet TTA-UCNPs. The amphiphilic polymer (F-127) not only enhanced the water solubility of silica TTA-UCNPs, but also provided a host to load the prodrug (Cou-C). In order to achieve far-red light cleavage of the prodrug, the metal-free BODIPY based photosensitizers (BDP-F) were prepared. The photosensitizers have strong absorption in the far red region, robust photostability and long triplet excited lifetime. In addition, the 9-phenylanthance (PEA) is the emitter due to their high deep blue fluorescence quantum yield. In addition, the upconversion spectrum is overlain with the absorption of Cou-C. When combined with BDP-F and PEA, the bright upconversion deep blue emission was observed upon the far red LED irradiation. The prodrug of Cou-C re-absorbed the upconversion and photocleaved the bond, leading to chemotherapy drug release from the nanodroplet nanoparticles. [71] The nanocomposites not only presented the obvious cancer cells growth inhibition but also showed significant tumor inhibition *in vivo*. This study provides a platform for the development of new biophotonic applications with to TTA-UCNPs.

2.5 Metal-organic frameworks (MOFs) based TTA-UCNPs.—Metal-organic frameworks (MOFs) have attracted widespread attention in biomedicine in recent years because of their structural diversity, easy preparation process, and good water solubility. [72] Furthermore, MOFs provided a flexible platform to control the ligand oritentation and ligand energy transfer on the molecular level. In addition, precise control of the distance of the chromophore can efficiently avoid the aggregation -induced fluorescence quenching in the MOFs.[73–80] Harnessing the advantages of MOFs, one can begin the development of TTA-UC MOFs to create a new type of upconversion material. As shown in Figure 12, Park *et al.* reported a low toxicity TTA-UC MOF and applied in *in vivo* bioimaging. In these TTA-UC MOFs, the emitter 4, 4-(9, 10-anthracenediyl) dibenzoic acid (DCDPA) is linked to construct a Zr-MOF. The photosensitizer Pd (II)-meso-tetrakis (4-carboxyphenyl) porphyrin (Pd-TCPP) was incorporated into a water stable Zr-MOF scaffold. In this TTA-UC MOFs, the coordination induced supramolecular self-assembly can efficiently tune the distance emitters and photosensitizers so as to decrease the dye aggregation induced the upconversion quenching. In addition, the orderly self-assembly of emitters and photosensitizers are beneficial to triplet-triplet energy migration, so that improve the upconversion quantum yield under low power intensity irradiation. Meanwhile, the TTA-UC MOFs presented high upconversion quantum yield by tuning the ratio of DCDPA and Pd-TCPP under low power light irradiation. In addition, the efficient triplet-triplet energy diffusion was observed in these TTA-UC MOFs, a feature which is beneficial in improving the upconversion efficiency. Finally, under low power excitation intensity, the TTA-UC MOF contrast agent was achieved with lymph node imaging with a high signal-to-noise ratio *in vivo*. [81]

Metal coordination supramolecular structure can not only generate the 3D TTA-UC MOFs, but also construct the one-dimensional (1D) chain structure. As shown in Figure 13, Hosoyamada *et al.* utilized the [Al (An)$_2$(OH)]$_n$ called MIL-53 as a template to construct the

TTA-UC MOFs. In these TTA-UC MOFs, the photosensitizer is platinum coordinated porphyrin (Por) and the emitter is DPA. The carboxylate groups were coordinated with Al^{3+} ions to form one dimensional lipophilic coordination copolymers. After the excitation, the efficient triplet-triplet energy migration was able to be observed. [82]

3. Conclusions

In summary, the design and preparation of TTA-UCNPs were recently explored. A series of new types of TTA-UCNPs were developed for their potential application in bioimaging and photoactivated drug release. As discussed here, these TTA-UCNPs (liposome coated TTA-UCNPs, polymer encapsulated TTA-UCNPs, silica-coated TTA-UCNPs, nanodroplet based TTA-UCNPs and TTA-UC MOFs, summarized in Table 1) show huge potential for next-generation biocompatible upconversion agents for biological applications. The TTA-UCNPs offer various advantages, such as 1) high upconversion quantum yield and outstanding light absorption coefficient, as well as biocompatibility for organism; 2) low power intensity excitation which is vital for bio-imaging *in vitro* and *in vivo*; and 3) broad and intensive absorption, and tunable upconversion wavelength as well as excellent photostability of TTA-UCNPs. Benefited from these unique properties, TTA-UCNPs provide a robust platform to develop the novel bioimaging and cancer therapy methods.

Despite the exciting biological applications realized by TTA-UCNPs, a number of challenges remain in regard to these existing TTA-UCNPs. For example, the anti-Stokes shift of existing TTA-UCNPs is typically suboptimal and the ideal upconversion nanoparticles should have a large anti-stokes shift, such as NIR to blue or UV range. Furthermore, the small and uniformly sized TTA-UCNPs are not readily available, which however is vital for biological applications. In addition, it is imperative that the surfaces of existing TTA-UCNPs are not able to be easily bioconjugated with other molecules. Therefore, the creation of new effective NIR absorbing photosensitizers in conjunction with TTA system would be beneficial to realize the NIR to visible light upconversion to expand the anti-Stokes shift in TTA-UC for more practical deep-tissue biological applications. Moreover, the development of new strategy to overcome oxygen quenching is greatly anticipated to improve the TTA upconversion quantum yield and brightness, particularly in context of aqueous solution. Conquering each of these challenges will provide new opportunities for TTA-UCNPs in biological applications such as for cancer therapy and neuron activation.

Acknowledgements

Reference:

[1]. Chen G, Qiu H, Prasad PN, Chen X. Upconversion nanoparticles: design, nanochemistry, and applications in theranostics, Chem. Rev 114 (2014) 5161–5214. [PubMed: 24605868]

[2]. Zhou J, Liu Q, Feng W, Sun Y, Li F. Upconversion luminescent materials: advances and applications, Chem. Rev 115 (2015) 395–465. [PubMed: 25492128]

[3]. Tu L, Liu X, Wu F, Zhang H. Excitation energy migration dynamics in upconversion nanomaterials, Chem. Soc. Rev 44 (2015) 1331–1345. [PubMed: 25223635]

[4] (a). Chen G, Ågren H, Ohulchanskyy TY, Prasad PN. Light upconverting core-shell nanostructures: nanophotonic control for emerging applications, Chem. Soc. Rev 44 (2015) 1680–1713. [PubMed: 25335878] (b)Liu J, Bu W, Pan L, Shi J. NIR-triggered anticancer drug delivery by upconverting nanoparticles with integrated azobenzene-modified mesoporous silica, Angew. Chem 125 (2013) 4471–4475;(c)Xing H, Bu W, Zhang S, Zheng X , Li M, Chen F, He Q, Zhou L, Peng W, Hua Y, Shi J. Multifunctional nanoprobes for upconversion fluorescence, MR and CT trimodal imaging, Biomaterials 33 (2012) 1079–1089; [PubMed: 22061493] (c)Liu Y, Meng X, Bu W, Upconversion-based photodynamic cancer therapy. Coordination Chemistry Reviews 379 (2019) 82–98.

[5]. Zhou J, Liu Z, Li F. Upconversion nanophosphors for small-animal imaging, Chem. Soc. Rev 41 (2012) 1323–1349. [PubMed: 22008740]

[6] (a). Shikha S, Salafi T, Cheng J, Zhang Y. Versatile design and synthesis of nano-barcodes, Chem. Soc. Rev 46 (2017) 7054–7093; [PubMed: 29022018] (b)Yang D, Ma P, Hou Z, Cheng Z, Li C , Lin J. Current advances in lanthanide ion (Ln3+)-based upconversion nanomaterials for drug delivery. Chem. Soc. Rev 44 (2015), 1416–1448; [PubMed: 24988288] (c)Gai S, Li C, Yang P, Lin J. Recent progress in rare earth micro/nanocrystals: soft chemical synthesis, luminescent properties, and biomedical applications. Chem. Rev 114 (2014) 2343–2389. [PubMed: 24344724]

[7]. Dong H, Du S-R, Zheng X-Y, Lyu G-M, Sun L-D, Li L-D. Lanthanide nanoparticles: From design toward bioimaging and therapy, Chem. Rev 115 (2015) 10725–10815. [PubMed: 26151155]

[8]. Chen G, Roy I, Yang C, Prasad PN. Nanochemistry and nanomedicine for nanoparticle-based diagnostics and therapy, Chem. Rev 116 (2016) 2826–2885. [PubMed: 26799741]

[9]. Peng H-Q, Niu L-Y, Chen Y-Z, Wu L-Z, Tung C-H, Yang Q-Z. Biological applications of supramolecular assemblies designed for excitation energy transfer, Chem. Rev 115 (2015) 7502–7542. [PubMed: 26040205]

[10]. Zhao J, Ji S, Guo H. Triplet–triplet annihilation based upconversion: from triplet sensitizers and triplet acceptors to upconversion quantum yields, RSC Adv 1 (2011) 937–950.

[11]. Zhao J, Wu W, Sun J, Guo S. Triplet photosensitizers: from molecular design to applications, Chem. Soc. Rev 42 (2013) 5323–5351. [PubMed: 23450221]

[12]. Zhao J, Xu K, Yang W, Wang Z, Zhong F. The triplet excited state of Bodipy: formation, modulation and application, Chem. Soc. Rev 44 (2015) 8904–8939. [PubMed: 26465741]

[13]. Zhu X, Su Q, Feng W, Li F. Anti-Stokes shift luminescent materials for bio-applications, Chem. Soc. Rev 46 (2017) 1025–1039. [PubMed: 27966684]

[14]. Filatov MA, Baluschevb S, Landfester K. Protection of densely populated excited triplet state ensembles against deactivation by molecular oxygen, Chem. Soc. Rev 45 (2016) 4668–4689. [PubMed: 27277068]

[15]. Baluschev S, Katta K, Avlasevich Y, Landfester K. Annihilation upconversion in nanoconfinement: solving the oxygen quenching problem, Mater. Horiz 3 (2016) 478–486.

[16]. Vadrucci R, Weder C, Simon YC. Organogels for low-power light upconversion, Mater. Horiz 2 (2015) 120–124.

[17]. Ji S, Guo H, Wu W, Wu W, Zhao J. Ruthenium (II) polyimine-coumarin dyad with non-emissive 3IL excited state as sensitizer for triplet-triplet annihilation based upconversion, Angew. Chem. Int. Ed 50 (2011) 8283–8286.

[18]. Lu Y, Wang J, McGoldrick N, Cui X, Zhao J, Caverly C, et al., Iridium (III) complexes bearing pyrene-functionalized 1,10-phenanthroline ligands as highly efficient sensitizers for triplet-triplet annihilation upconversion, Angew. Chem. Int. Ed 55 (2016) 14688–14692.

[19]. Borisov SM, Saf R, Fischer R, Klimant I. Synthesis and properties of new phosphorescent red light-excitable platinum (II) and palladium (II) complexes with Schiff bases for oxygen sensing and triplet-triplet annihilation-based upconversion, Inorg. Chem 52 (2013) 1206–1216. [PubMed: 23231719]

[20]. Yi X, Zhao J, Sun J, Guo S, Zhang H. Visible light-absorbing rhenium(I) tricarbonyl complexes as triplet photosensitizers in photooxidation and triplet-triplet annihilation upconversion, Dalton Trans 42 (2013) 2062–2074. [PubMed: 23178459]

[21]. Han J, Duan P, Li X, Liu M. Amplification of circularly polarized luminescence through triplet-triplet annihilation-based photon upconversion, J. Am. Chem. Soc 139 (2017) 9783–9786. [PubMed: 28686421]

[22]. Kim H-l, Kwon OS, Kim S, Choi W, Kim J-H. Harnessing low energy photons (635 nm) for the production of H2O2 using upconversion nanohybrid photocatalysts, Energy Environ. Sci 9 (2016) 1063–1073.

[23]. Liu Q, Xu M, Yang T, Tian B, Zhang X, Li F. Highly photostable near-IR-excitation upconversion nanocapsules based on triplet-triplet annihilation for in vivo bioimaging application, ACS Appl. Mater. Interfaces, 10 (2018) 9883–9888. [PubMed: 29425018]

[24]. Xu K, Zhao J, Escudero D, Mahmood Z, Jacquemin D. Controlling triplet–triplet annihilation upconversion by tuning the PET in aminomethyleneanthracene derivatives, J. Phys. Chem C, 119 (2015) 23801–23812.

[25]. Duan P, Yanai N, Nagatomi H, Kimizuka N. Photon upconversion in supramolecular gel matrixes: spontaneous accumulation of light-harvesting donor-acceptor arrays in nanofibers and acquired air stability, J. Am. Chem. Soc 137 (2015) 1887–1894. [PubMed: 25599418]

[26]. Duan P, Yanai N, Kimizuka N. Photon upconverting liquids: matrix-free molecular upconversion systems functioning in air, J. Am. Chem. Soc 135 (2013) 19056–19059. [PubMed: 24328197]

[27]. Singh-Rachford TN, Haefele A, Ziessel R, Castellano FN. Boron dipyrromethene chromophores: next generation triplet acceptors/annihilators for low power upconversion schemes, J. Am. Chem. Soc 130 (2008) 16164–16165. [PubMed: 18998677]

[28]. Wang C, Zhang Q, Wang X, Chang H, Zhang S, Tang Y et al.,. Dynamic modulation of enzyme activity by near-infrared light, Angew. Chem. Int. Ed 56 (2017) 6767–6772.

[29]. Jing T, Dai Y, Wei W, Ma X, Huang B. Near-infrared photocatalytic activity induced by intrinsic defects in Bi2MO6 (M = W, Mo), Phys. Chem. Chem. Phys 16 (2014) 18596–18604. [PubMed: 25075587]

[30]. Wang Z, Zhao J, Barbon A, Toffoletti A, Liu Y, An Y, et al., Radical-enhanced intersystem crossing in new Bodipy derivatives and application for efficient triplet-triplet annihilation upconversion, J. Am. Chem. Soc 139 (2017) 7831–7842. [PubMed: 28524657]

[31]. Wu W, Guo H, Wu W, Ji S, Zhao J. Organic triplet sensitizer library derived from a single chromophore (BODIPY) with long-lived triplet excited state for triplet-triplet annihilation based upconversion, J. Org. Chem 76 (2011) 7056–7064. [PubMed: 21786760]

[32]. Zhang C, Zhao J, Wu S, Wang Z, Wu W, Ma J, et al.,. Intramolecular RET enhanced visible light-absorbing bodipy organic triplet photosensitizers and application in photooxidation and triplet-triplet annihilation upconversion, J. Am. Chem. Soc 135 (2013) 10566–10578. [PubMed: 23790008]

[33]. Hwang JY, Li Z, Loh XJ. Small molecule therapeutic-loaded liposomes as therapeutic carriers: from development to clinical applications, RSC Adv 6 (2016) 70592–70615.

[34]. Grimaldi N, Andrade F, Segovia N, Ferrer-Tasies L, Sala S, Veciana ac J., Ventosa N. Lipid-based nanovesicles for nanomedicine, Chem. Soc. Rev 45 (2016) 6520–6545. [PubMed: 27722570]

[35]. Chen C, Zhu S, Huang T, Wang S, Yan X. Analytical techniques for single-liposome characterization, Anal. Methods, 5 (2013) 2150–2157.

[36]. Askes SHC, Bahreman A, Bonnet S. Activation of a photodissociative ruthenium complex by triplet-triplet annihilation upconversion in liposomes, Angew. Chem. Int. Ed 53 (2014) 1029–1033.

[37]. Gulzar A, Xu J, Yang P, He F, Xu L. Upconversion processes: versatile biological applications and biosafety, Nanoscale, 9 (2017) 12248–12282. [PubMed: 28829477]

[38]. Wong H-T, Tsang M-K, Chan C-F, Wong K-L, Fei B, Hao J. In vitro cell imaging using multifunctional small sized KGdF4:Yb3+,Er3+ upconverting nanoparticles synthesized by a one-pot solvothermal process, Nanoscale, 5 (2013) 3465–3473. [PubMed: 23475279]

[39]. Hemmer E, Acosta-Mora P, Méndez-Ramos J, Fischer S. Optical nanoprobes for biomedical applications: shining a light on upconverting and near-infrared emitting nanoparticles for imaging, thermal sensing, and photodynamic therapy, J. Mater. Chem. B, 5 (2017) 4365–4392.

[40]. Mattiello S, Monguzzi A, Pedrini J, Sassi M, Villa C, Torrente Y, et al., Self-assembled dual dye −doped nanosized micelles for high−contrast up−conversion bioimaging, Adv. Funct. Mater 26 (2016) 8447–8454.

[41]. Kouno H, Ogawa T, Amemori S, Mahato P, Yanai N, Kimizuka N. Triplet energy migration-based photon upconversion by amphiphilic molecular assemblies in aerated water, Chem. Sci 7 (2016) 5224–5229. [PubMed: 30155172]

[42]. Poznik M, Faltermeier U, Dick B, König B. Light upconverting soft particles: triplet–triplet annihilation in the phospholipid bilayer of self-assembled vesicles, RSC Adv 6 (2016) 41947–41950.

[43]. (a). Yildirim A, Chattaraj R, Blum NT, Goldscheitter GM, Goodwin AP. Stable encapsulation of air in mesoporous silica nanoparticles: fluorocarbon-free nanoscale ultrasound contrast agents, Adv. Healthcare Mater 5 (2016), 1290–1298.(b)Niu D, Li Y, Shi J. Silica/organosilica cross-linked block copolymer micelles: a versatile theranostic platform. Chem. Soc. Rev 2017, 46 (2017) 569–585.

[44]. Ma X, Nguyen KT, Borah P, Ang CY, Zhao Y. Functional silica nanoparticles for redox-triggered drug/ssDNA co-delivery, Adv. Healthcare Mater 1 (2012) 690–697.

[45]. Huo Q, Liu J, Wang L-Q, Jiang Y, Lambert TN, Fang E. A new class of silica cross-linked micellar core-shell nanoparticles, J. Am. Chem. Soc 128 (2006) 6447–6453. [PubMed: 16683810]

[46]. Caltagirone C, Bettoschi A, Garau A, Montis R. Silica-based nanoparticles: a versatile tool for the development of efficient imaging agents, Chem. Soc. Rev 44 (2015) 4645–4671. [PubMed: 25406516]

[47]. Montalti M, Prodi L, Rampazzo E, Zaccheroni N. Dye-doped silica nanoparticles as luminescent organized systems for nanomedicine, Chem. Soc. Rev 43 (2014) 4243–4268. [PubMed: 24643354]

[48]. Bonacchi S, Genovese D, Juris R, Montalti M, Prodi L, Rampazzo E, et al.,. Luminescent silica nanoparticles: extending the frontiers of brightness, Angew. Chem. Int. Ed 50 (2011) 4056–4066.

[49]. Liu Q, Yang T, Feng W, Li F. Blue-emissive upconversion nanoparticles for low-power-excited bioimaging in Vivo, J. Am. Chem. Soc 134 (2012) 5390–5397. [PubMed: 22369318]

[50]. Kwon OS, Kim J-H, Cho JK, Kim J-H. Triplet–triplet annihilation upconversion in CdS-Decorated SiO2 nanocapsules for sub-bandgap photocatalysis, ACS Appl. Mater. Interfaces 7 (2015) 318–325. [PubMed: 25522373]

[51]. Kwon OS, Song HS, Conde J, Kim H.-l., Artzi N, Kim J-H. Dual-color emissive upconversion nanocapsules for differential cancer bioimaging In Vivo, ACS Nano 10 (2016) 1512–1521. [PubMed: 26727423]

[52]. Trofymchuk K, Prodi L, Reisch A, Mély Y, Altenhöner K, Mattay J. Exploiting fast exciton diffusion in dye-doped polymer nanoparticles to engineer efficient photoswitching, J. Phys. Chem. Lett 6 (2015) 2259–2264. [PubMed: 26266601]

[53]. Wu C, Zheng Y, Szymanski C, McNeill J. Energy transfer in a nanoscale multichromophoric system: fluorescent dye-doped conjugated polymer nanoparticles, J. Phys. Chem C, 112 (2008) 1772–1781.

[54]. Li S, Shen X, Li L, Yuan P, Guan Z, Yao SQ, et al.,. Conjugated-polymer-based red-emitting nanoparticles for two-photon excitation cell imaging with high contrast, Langmuir, 30 (2014) 7623–7627. [PubMed: 24967827]

[55]. Jana B, Bhattacharyya S, Patra A. Functionalized dye encapsulated polymer nanoparticles attached with a BSA scaffold as efficient antenna materials for artificial light harvesting, Nanoscale, 8 (2016), 16034–16043. [PubMed: 27546792]

[56]. Dryza V, Smith TA, Bieske EJ. Blue to near-IR energy transfer cascade within a dye-doped polymer matrix, mediated by a photochromic molecular switch, Phys. Chem. Chem. Phys 18 (2016) 5095–5098. [PubMed: 26816320]

[57]. Wu C, Chiu DT. Highly fluorescent semiconducting polymer dots for biology and medicine, Angew. Chem. Int. Ed 52 (2013) 3086–3109.

[58]. Kim J-H, Kim J-H. Triple-emulsion microcapsules for highly efficient multispectral upconversion in the aqueous phase, ACS Photonics, 2 (2015) 633–638.

[59]. Wohnhaas C, Friedemann K, Busko D, Landfester K, Baluschev S, Crespy D. All organic nanofibers as ultralight versatile support for triplet–triplet annihilation upconversion, ACS Macro Lett 2 (2013) 446–450.

[60]. Kim J-H, Deng F, Castellano FN, Kim J-H. Red-to-Blue/Cyan/Green upconverting microcapsules for aqueous-and dry-phase color tuning and magnetic sorting, ACS Photonics, 1 (2014) 382–388.

[61]. Kang J-H, Lee SS, Guerrero J, Fernandez-Nieves A, Kim S-H, Reichmanis E. Ultrathin double −shell capsules for high performance photon upconversion, Adv. Mater 29 (2017) 1606830.

[62]. Kim J-H, Kim J-H. Encapsulated triplet–triplet annihilation-based upconversion in the aqueous phase for sub-band-gap semiconductor photocatalysis, J. Am. Chem. Soc 134 (2012) 17478–17481. [PubMed: 23062012]

[63]. Wohnhaas C, Mailänder V, Dröge M, Filatov MA, Busko D, Avlasevich Y. Triplet-triplet annihilation upconversion based nanocapsules for bioimaging under excitation by red and deep-red light, Macromol. Biosci 13 (2013) 1422–1430. [PubMed: 23868857]

[64]. Askes SHC, Pomp W, Hopkins SL, Kros A, Wu S, Schmidt T, Bonnet S. Imaging upconverting polymersomes in cancer cells: biocompatible antioxidants brighten triplet-triplet annihilation upconversion, Small 12 (2016) 5579–5590. [PubMed: 27571308]

[65]. Wang W, Liu Q, Zhan C, Barhoumi A, Yang T, Wylie RG et al.,. Efficient triplet–triplet annihilation-based upconversion for nanoparticle phototargeting, Nano Lett 15 (2015) 6332–6338. [PubMed: 26158690]

[66]. Liu Q, Wang W, Zhan C, Yang T, Kohane DS. Enhanced precision of nanoparticle phototargeting in vivo at a safe irradiance, Nano Lett 16 (2016) 4516–4520. [PubMed: 27310596]

[67]. Liu Q, Yin B, Yang T, Yang Y, Shen Z, Yao P et al.,. A general strategy for biocompatible, high-effective upconversion nanocapsules based on triplet–triplet annihilation, J. Am. Chem. Soc 135 (2013) 5029–5037. [PubMed: 23464990]

[68]. Klán P, Šolomek T, Bochet CG, Blanc A, Givens R, Rubina M et al.,. Photoremovable protecting groups in chemistry and biology: reaction mechanisms and efficacy, Chem. Rev 113 (2013), 119–191. [PubMed: 23256727]

[69]. Kammari L, Šolomek T, Ngoy BP, Heger D, Klán P. Orthogonal photocleavage of a monochromophoric linker, J. Am. Chem. Soc 132 (2010) 11431–11433. [PubMed: 20684513]

[70]. Lin Q, Bao C, Cheng S, Yang Y, Ji W, Zhu L. Target-activated coumarin phototriggers specifically switch on fluorescence and photocleavage upon bonding to thiol-bearing protein, J. Am. Chem. Soc 134 (2012) 5052–5055. [PubMed: 22394079]

[71]. Huang L, Zhao Y, Zhang H, Huang K, Yang J, Han G. Expanding anti-stokes shifting in triplet-triplet annihilation upconversion for in vivo anticancer prodrug activation, Angew. Chem. Int. Ed 56 (2017) 14400–14404.

[72]. Chen W, Wu C. Synthesis, functionalization, and applications of metal–organic frameworks in biomedicine. Dalton Trans 47 (2018), 2114–2133; [PubMed: 29369314] (b)Rojas S, Devic T, Horcajada P. Metal organic frameworks based on bioactive components. J. Mater. Chem. B, 5 (2017) 2560–2573.

[73] (a). Stock N, Biswas S. Synthesis of Metal-Organic Frameworks (MOFs): Routes to Various MOF Topologies, Morphologies, and Composites, Chem. Rev 112 (2012), 933–969. [PubMed: 22098087] (b)Gagnon KJ, Perry HP, Clearfield A. Conventional and unconventional metal–organic frameworks based on phosphonate ligands: MOFs and UMOFs, Chem. Rev 112 (2012), 1034–1054. [PubMed: 22126609]

[74]. Schoedel A, Li M, Li D, O'Keeffe M, Yaghi OM. Structures of metal–organic frameworks with rod secondary building units, Chem. Rev 116 (2016) 12466–12535. [PubMed: 27627623]

[75]. Lee CY, Farha OK, Hong BJ, Sarjeant AA, Nguyen ST, Hupp JT. Light-harvesting metal–organic frameworks (MOFs): efficient strut-to-strut energy transfer in Bodipy and porphyrin-based MOFs, J. Am. Chem. Soc 133 (2011) 15858–15861. [PubMed: 21916479]

[76]. Kent CA, Mehl BP, Ma L, Papanikolas JM, Meyer TJ, Lin W. Energy transfer dynamics in metal−organic frameworks, J. Am. Chem. Soc 132 (2010) 12767–12769. [PubMed: 20735124]

[77]. Ullman AM, Brown JW, Foster ME, Léonard F, Leong K, Stavila V, Allendorf MD. Transforming MOFs for energy applications using the guest@MOF concept. Inorg. Chem 55 (2016), 7233–7249. [PubMed: 27399607]

[78]. Zhao X, Song X, Li Y, Chang Z, Chen L. Targeted construction of light-harvesting metal–organic frameworks featuring efficient host–guest energy transfer, ACS Appl. Mater. Interfaces, 10 (2018) 5633–5640. [PubMed: 29350906]

[79]. Park KC, Seo C, Gupta G, Kim J, Le CY. Efficient energy transfer (EnT) in pyrene−and porphyrin-based mixed-ligand metal–organic frameworks, ACS Appl. Mater. Interfaces, 9 (2017) 38670–38677. [PubMed: 29048158]

[80]. Park HJ, So MC, Gosztola D, Wiederrecht GP, Emery JD, Martinson ABF et al.,. Layer-by-layer assembled films of perylene diimide−and squaraine-containing metal–organic framework-like materials: Solar energy capture and directional energy transfer, ACS Appl. Mater. Interfaces, 8 (2016) 24983–24988. [PubMed: 27617568]

[81]. Park J, Xu M, Li F, Zhou H-C. 3D long-range triplet migration in a water-stable metal–organic framework for upconversion-based ultralow-power in vivo imaging, J. Am. Chem. Soc 140 (2018) 5493–5499. [PubMed: 29634258]

[82]. Hosoyamada M, Yanai N, Okumura K, Uchihashi T, Kimizuka N. Translating MOF chemistry into supramolecular chemistry: soluble coordination nanofibers showing efficient photon upconversion, Chem. Commun 54 (2018) 6828–6831.

PtOEP   **PdTPBP**   **PdPc(OBu)8**   **2,6-diiodio-BODIPY**

DPA   **Perylene**   **BDP-515**   **BDP-546**   **Rubene**
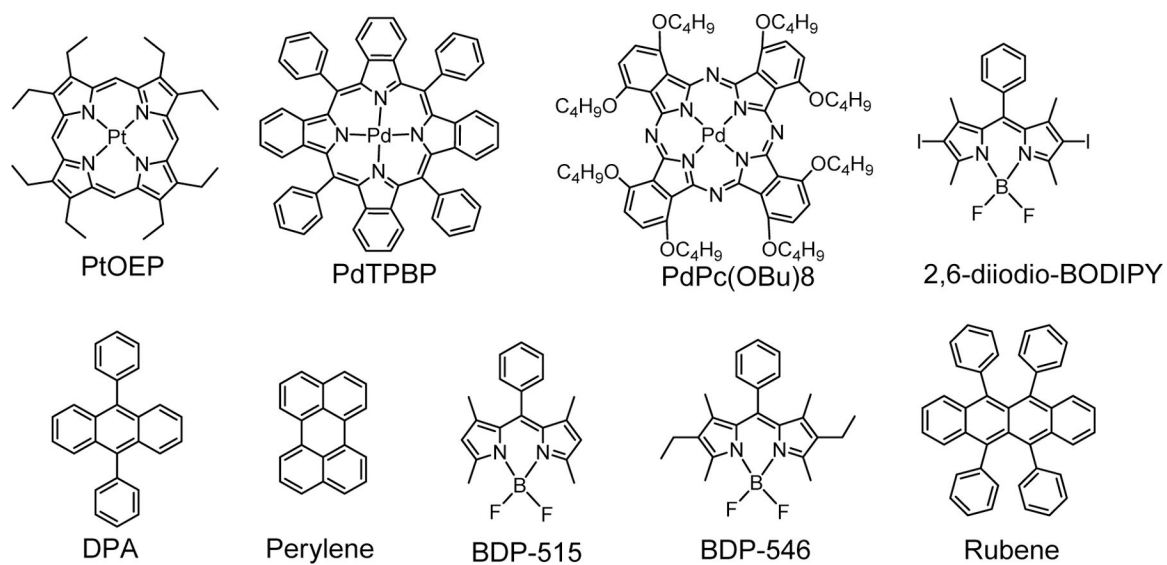
Figure 1.
The commercial photosensitizers (PtOEP, PdTPBP, PdPc (OBu)$_8$, 2,6-diiodio-BPDIPY) and emitters (DPA, perylene, BDP-515, BDP-546, and Rubene).
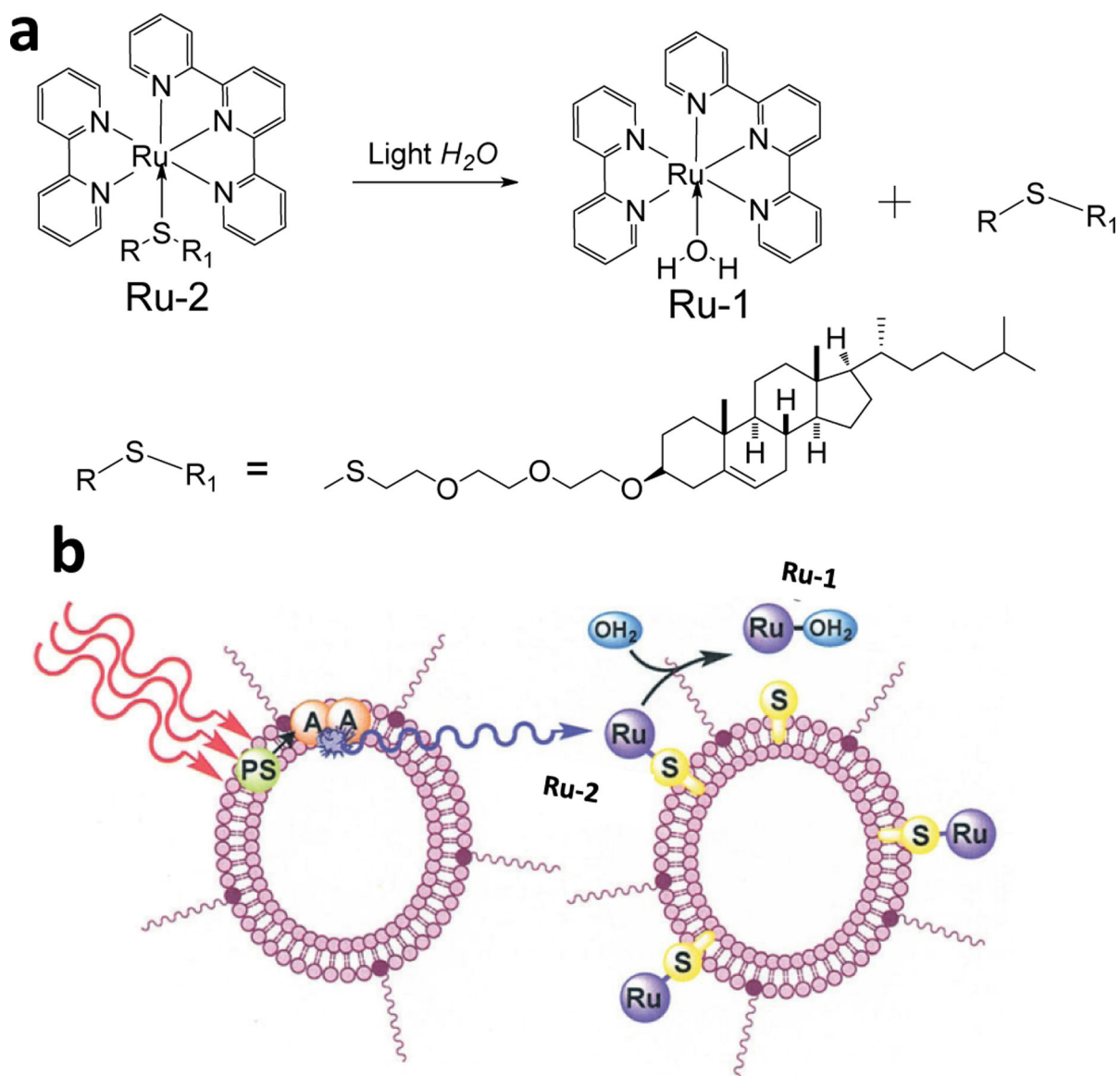
Figure 2.
(a) Molecular structures Ru-1 and Ru-2. (b) Schematic illustration the TTA-UC liposomes structure and TTA-UC trigger the Ru-1 releasing process with red light irradiation, $\lambda_{ex} = 630$ nm Reference 36
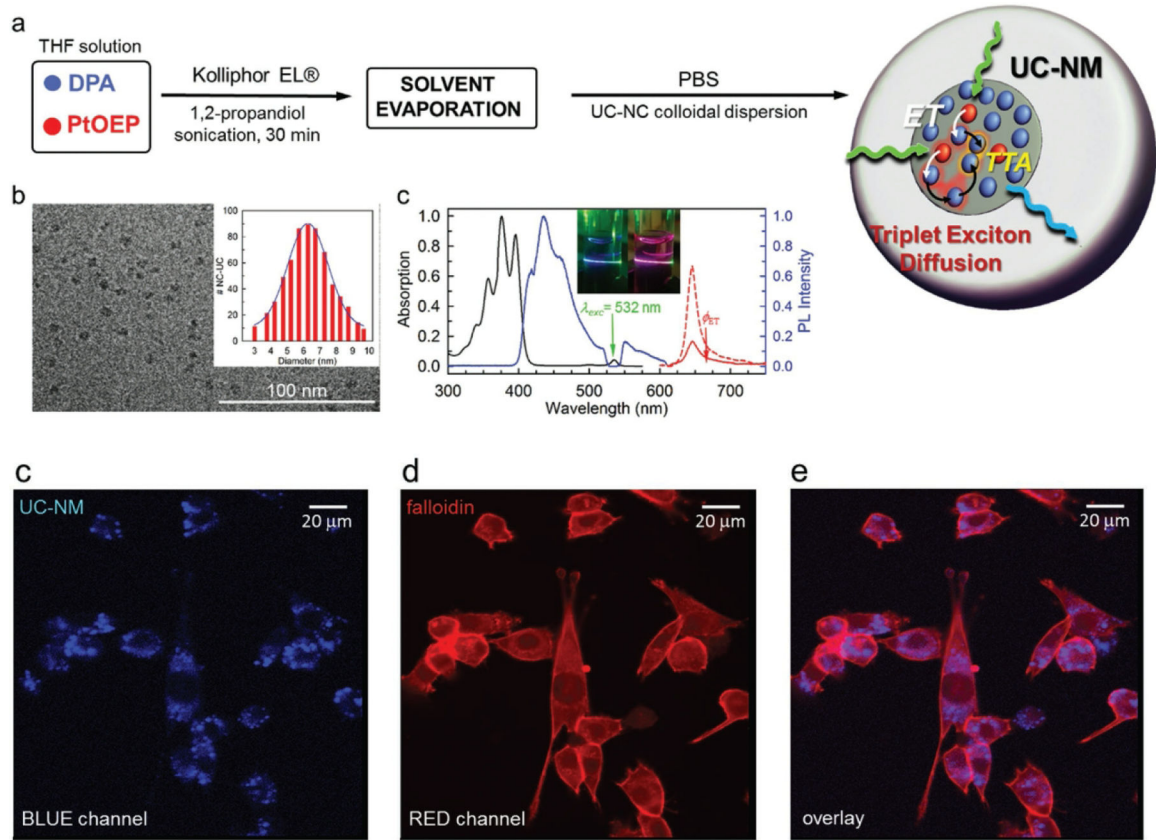
Figure 3.
Upper panel: (a) schematic illustration the preparation of the TTA-UCNPs containing PtOEP and DPA. (b) Cryo-TEM images of TTA-UC nanomicelles (c) UV-vis absorption spectra, TTA-UC emission spectra and phosphorescence emission spectrum of TTA-UC nanomicelles. Bottom panel (c-d) Confocal imaging of TTA-UC nanomicelles with 532 laser irradiation in 3T3 cell, (c) blue channel, (d) red channel and (d) overlay imaging.
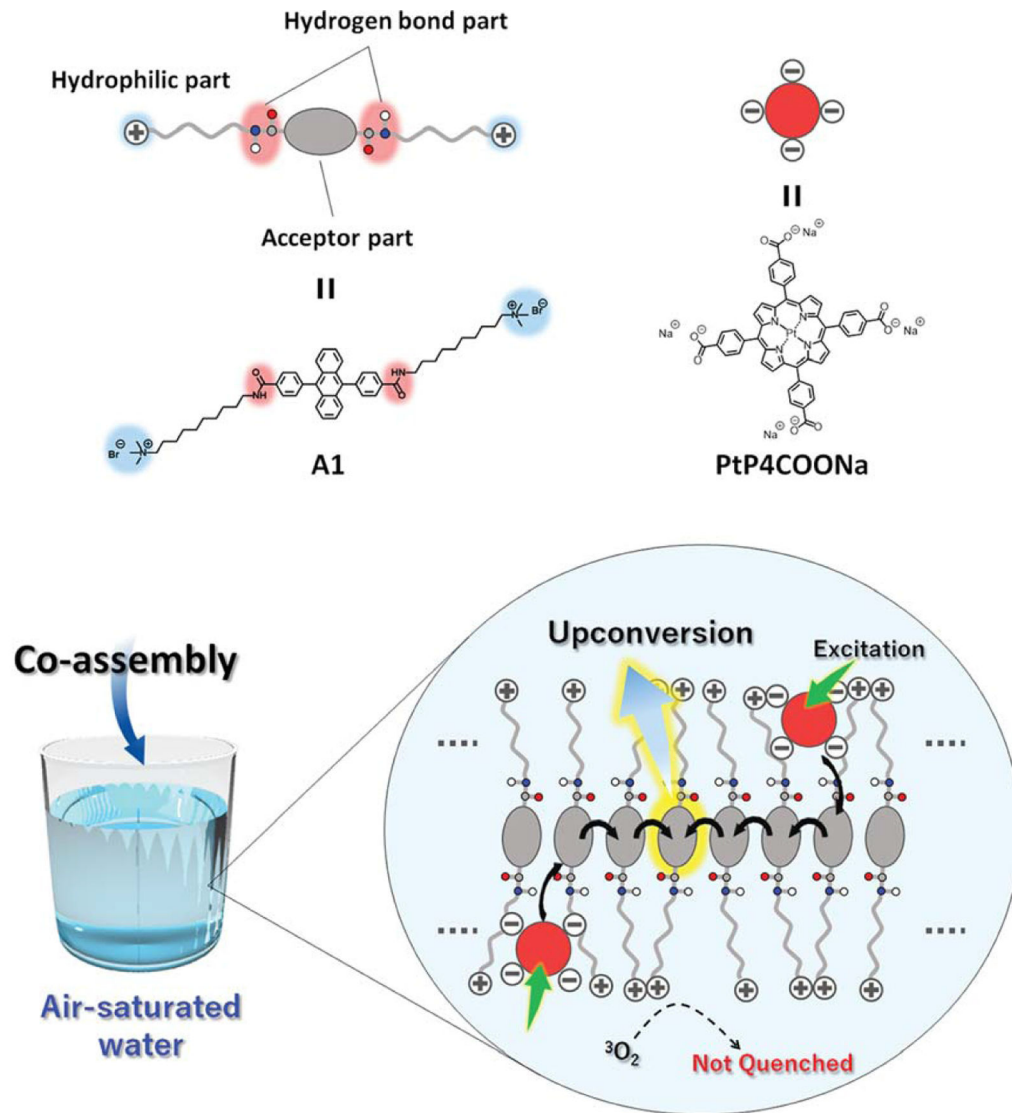
Figure 4.
Schematic illustration of formed the aqueous TEM-UC system process. Top panel: molecular structure of A-1 and PtP4COONa. Bottom panel: the A-1 and PtP4COONa by self-assembly generation the TEM-UC system in air-saturated water. Reference 41.
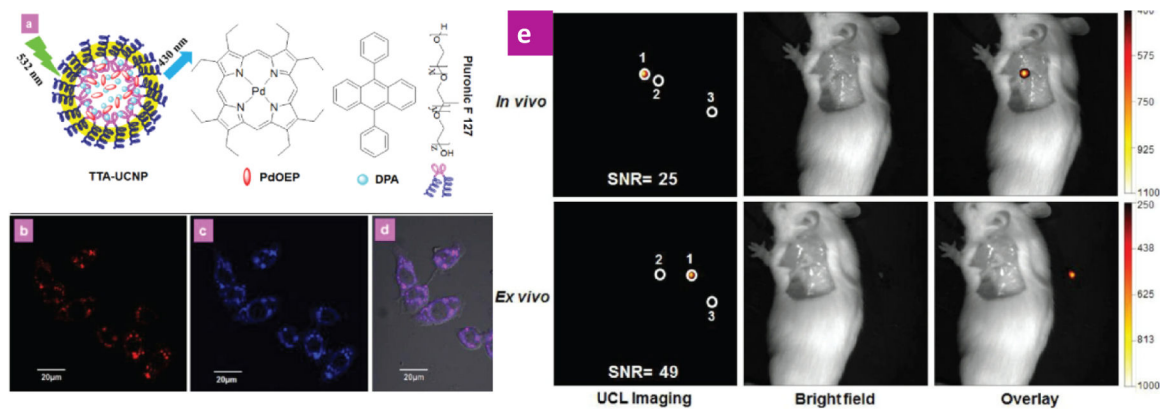
Figure 5.
(a) Schematic illustration of silica coated TTA-UCNPs, and molecular structure of PdOEP, DPA and F-127. (b, c) Fluorescence cell imaging (b, λ_{ex} = 543 nm, upconversion imaging) and (c, λ_{ex} = 405 nm, conventional fluorescence image) (d) the overlay of imaging of (b) and (c). (e) *In vivo* and *ex vivo* upconversion imaging by silica coated TTA-UCNPs as contrast agents. Reference 49.
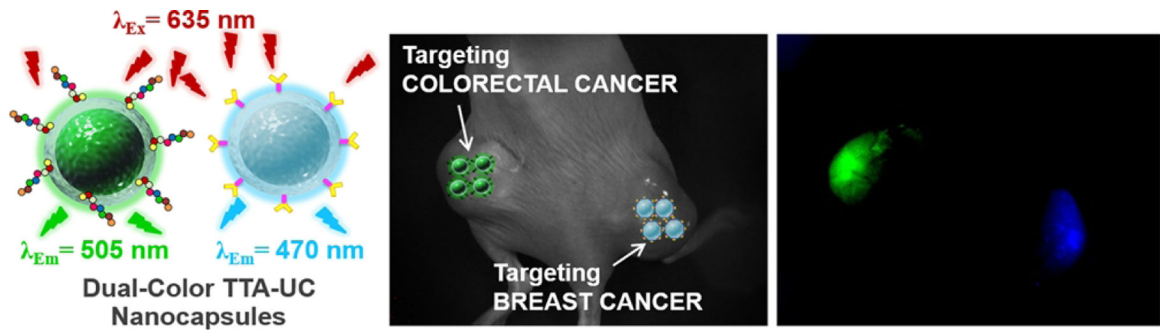
Figure 6.
Left: a schematic illustration of dual color silica-TTA-UCNPs. Right: mice bright field imaging of TTA-UCNPs and the blue and green upconversion emission for mice breast and colorectal tumor. Reference 51.
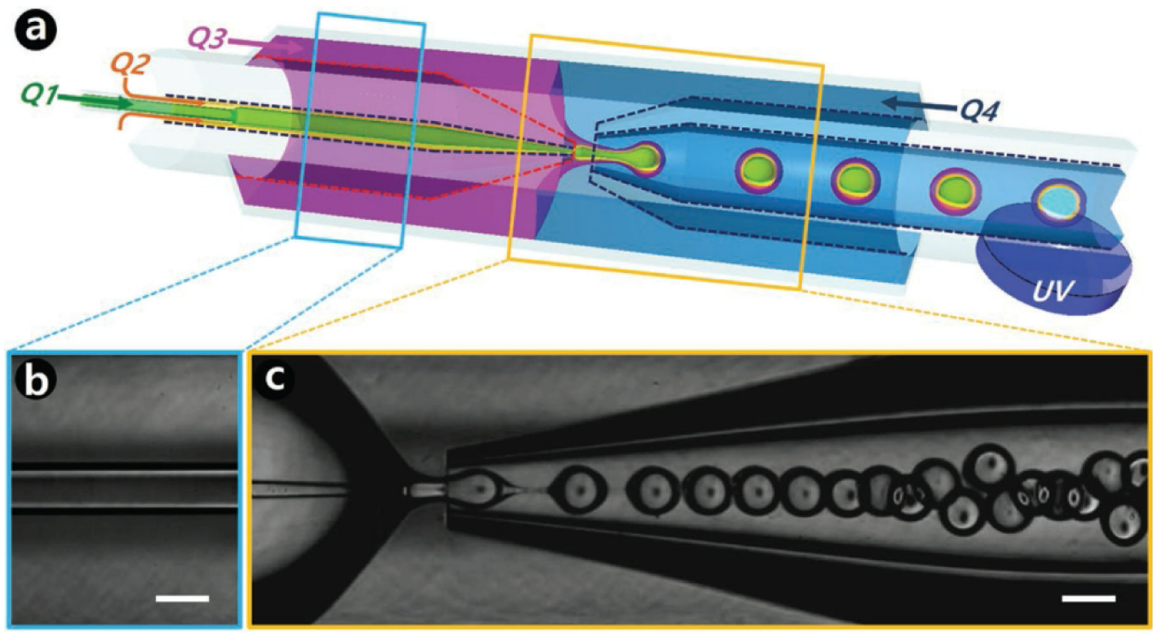
Figure 7.
(a) Schematic illustration of a glass capillary microfluidic device to synthesize the polymer encapsulated TTA-UCNPs. (b, c) High-speed optical microscopy observed the process preparation the polymer encapsulated TTA-UCNPs, scar bar is 200 μm.
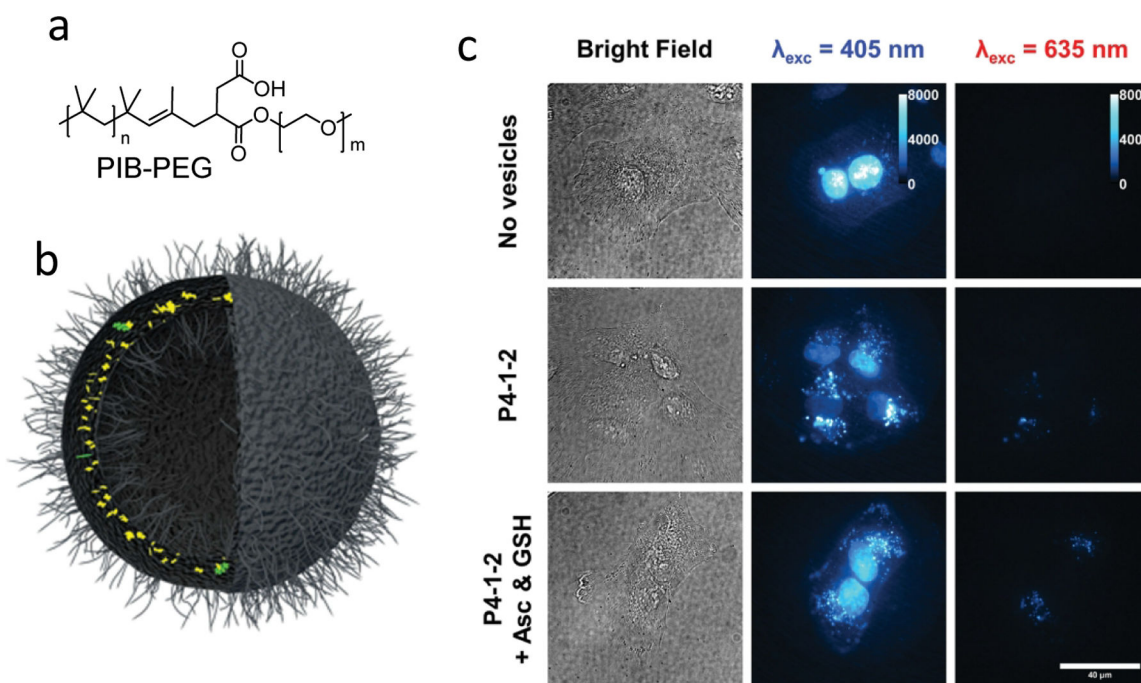
Figure 8.
Chemical structures of the PIB-PEG; (b) Schematic illustration of a PIB-PEG encapsulated TTA-UCNPs. (c) In vitro upconversion imaging in living A549 lung carcinoma cells under different conditions. Reference 64.
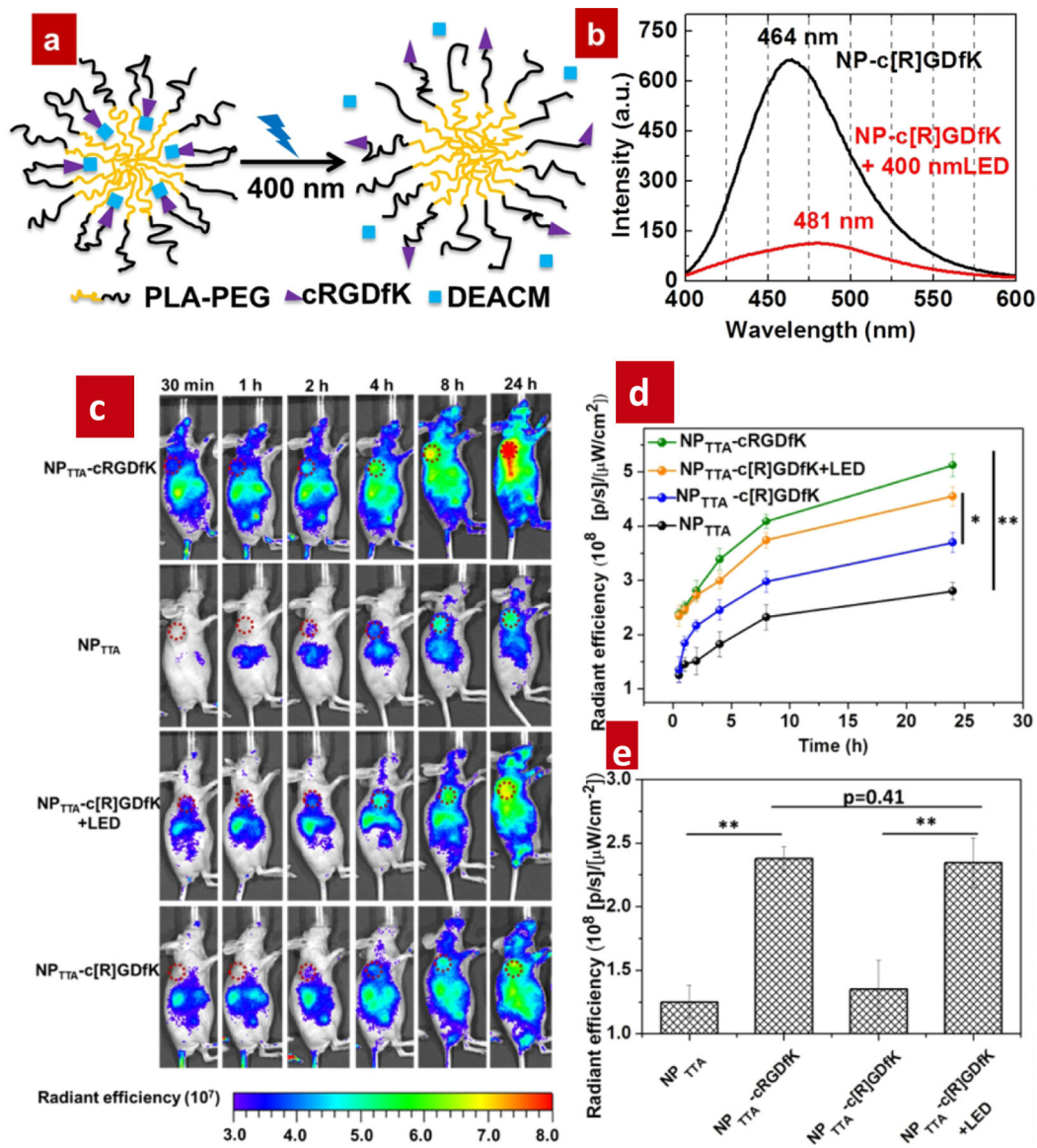
Figure 9.
(a) Schematic illustration the PLA-PEG coated TTA-UCNPs. (b) Fluorescence emission spectra of c-RGDfK under different condition (c) NP_{TTA}-c-RGDfK imaging in tumor-bearing mice under different conditions. (d) Quantitative analysis of the fluorescence intensity for TTA-UCNPs under different conditions. (e) Quantitative analysis the fluorescence intensity of tumor site under different conditions, $\lambda_{ex} = 530$ nm, PdOEP (photosensitizer), DPA (emitter) Reference 65–66
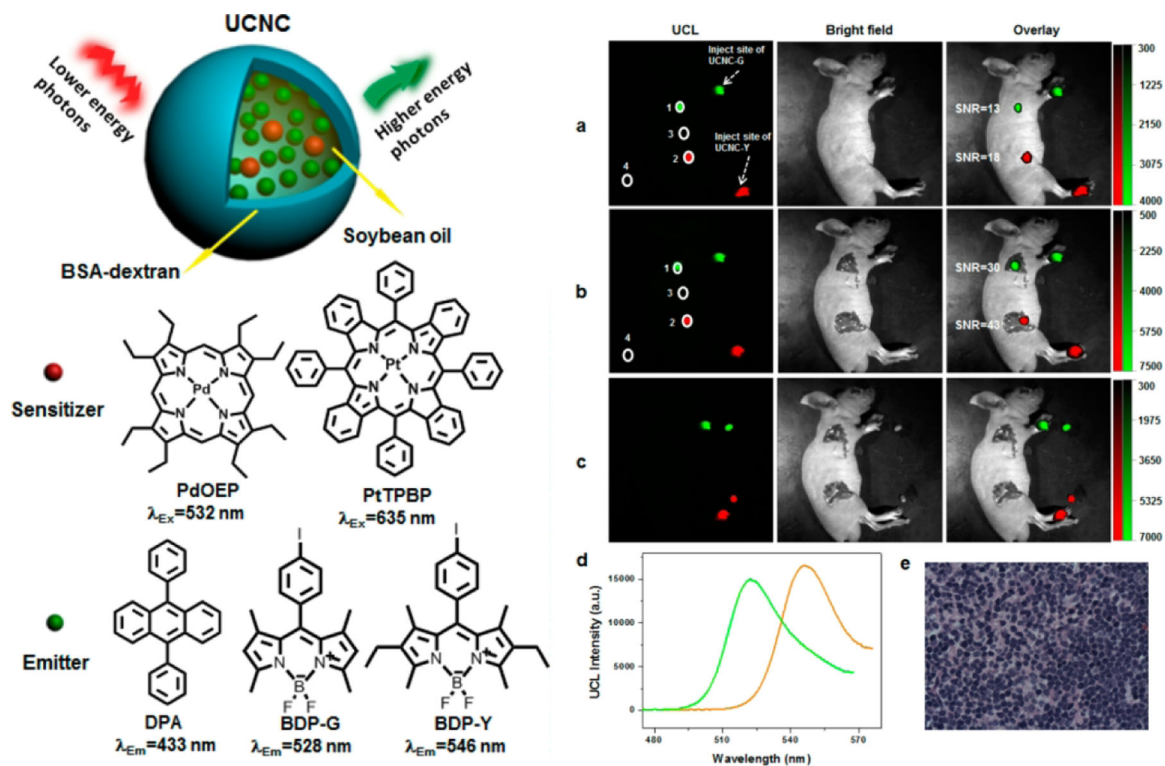
Figure 10.
Left: a schematic illustration of TTA-UC nanocapsules, and molecular structures of PdOEP, PtTPBP, DPA, BDP-G, and BDP-Y. Right: (a) *In vivo* lymphatic imaging of the living mouse (d) TTA-UC fluorescence spectra nanocapsules. (e) Hematoxylin and eosin (H&E) staining mice lymph node imaging. Reference 67.
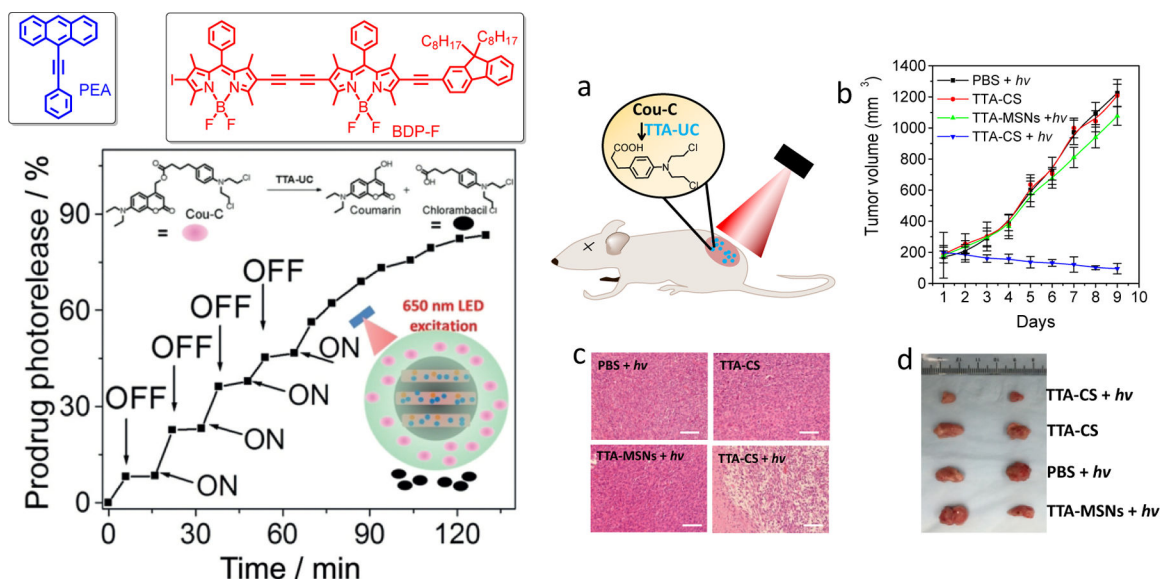
Figure 11.
Left up: chemical structure of PEA and BDP-F; Left down: The TTA-UC photoactivation of Cou-C from TTA-CS, Bottom inset: a schematic illustration of a TTA-UC-induced prodrug photoactivation process. Right (a) schematics illustration of the photoactivation (c) Hematoxylin and eosin (H&E) staining of tumor tissue sections from different treatment groups (d) Representative digital photos of tumors for the four groups of mice, excitation power intensity is 100 mW/cm^2, Reference 71.
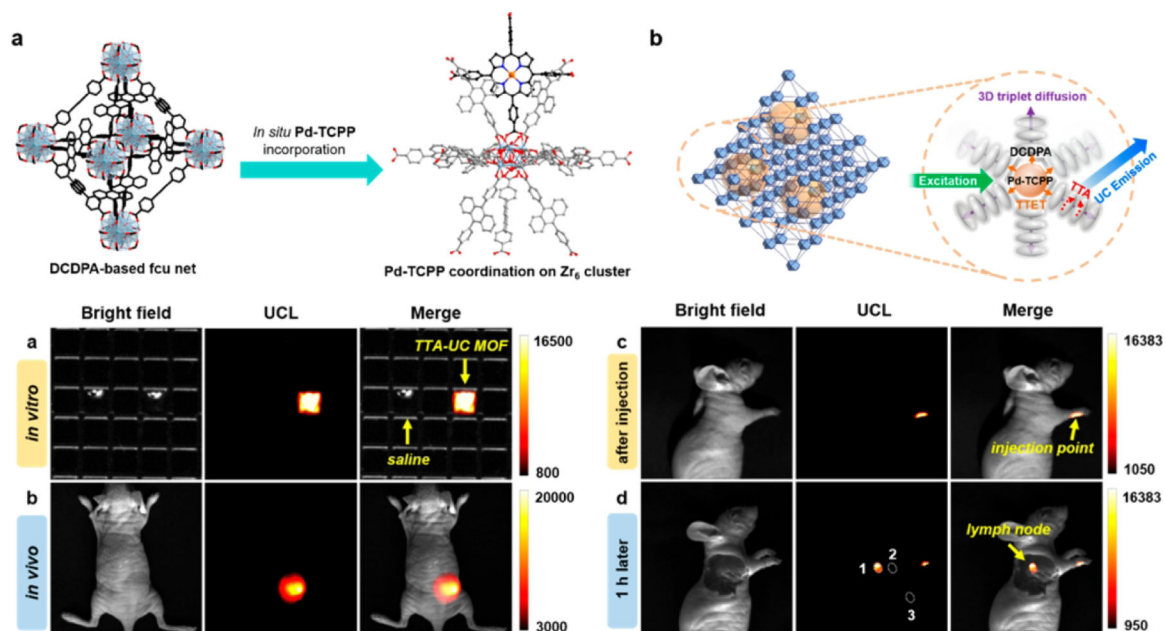
Figure 12.
Upper panel: (a) crystal structure of TTA-UC MOF. (b) Schematic illustration of PdTCPP energy transfer to emitters. Bottom panel: In vitro and in vivo imaging of TTA-UC MOF. (a) In vitro and (b) in vivo imaging with TTA-UC MOF. (c, d) In vivo lymph node imaging with TTA-UC MOF as an imaging contrast agent in living mice model, λ_{ex} = 532 nm Reference 81
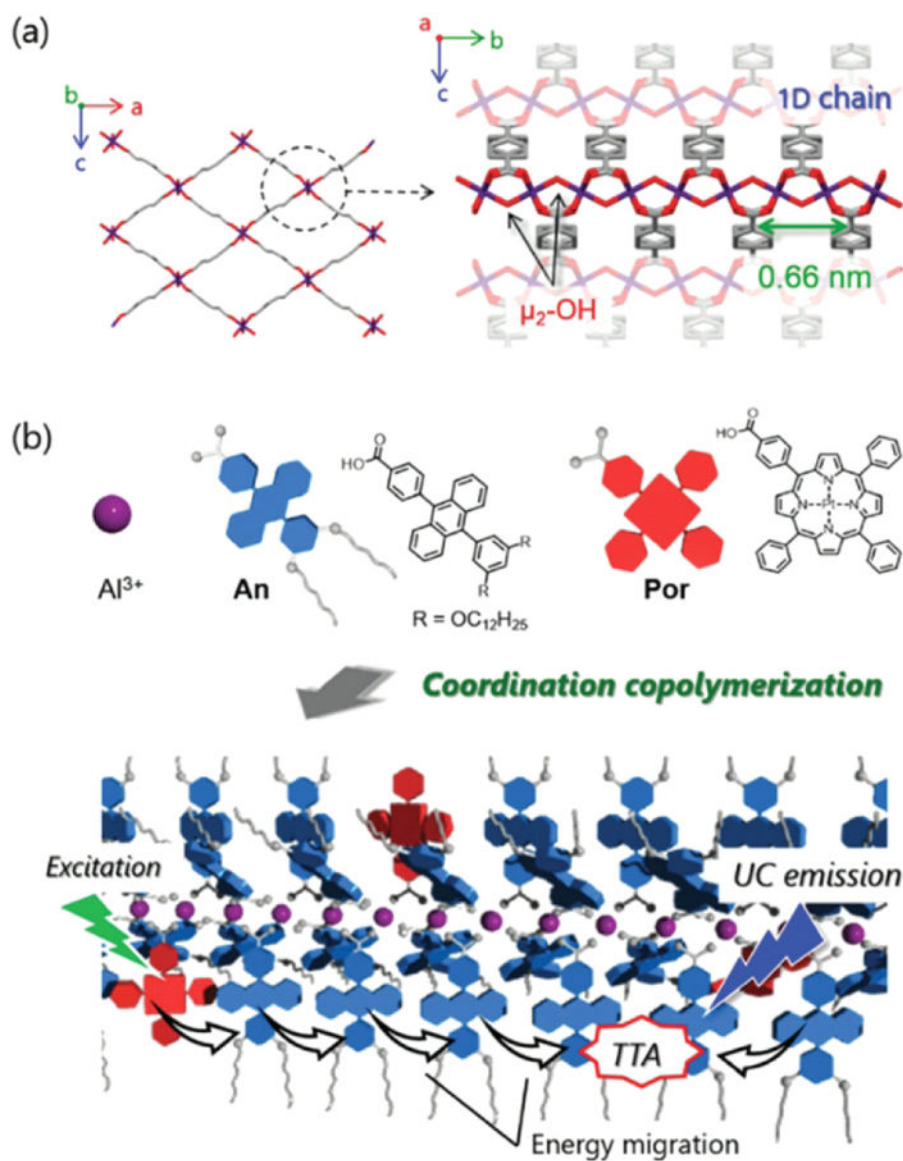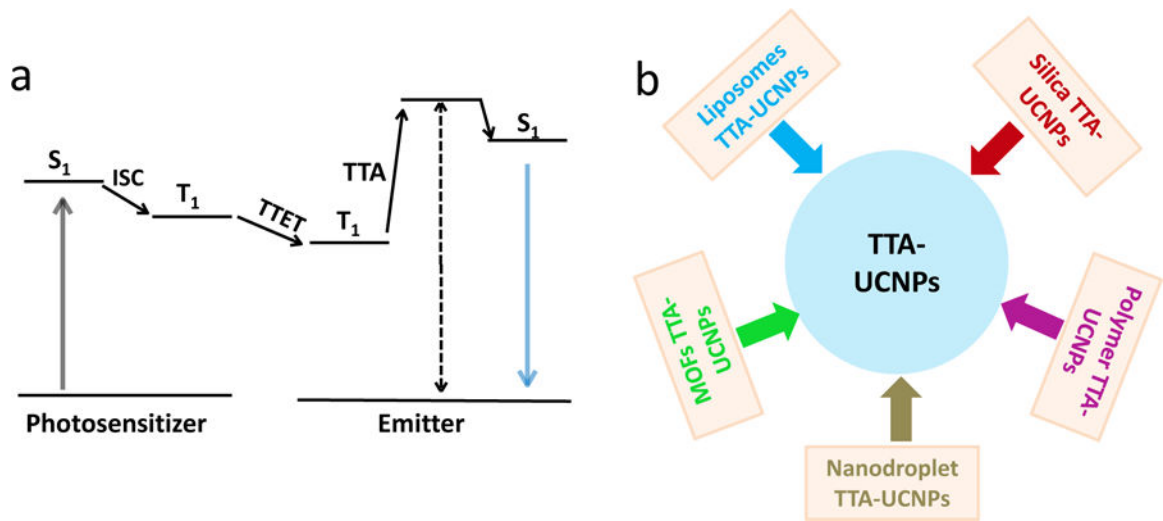
Figure 13.
(a) Crystal structure of MIL-53. (b) Molecular structures of An and Por, and schematic illustration of TTA-UC process in coordination copolymers, λ_{ex} = 515 nm Reference 82

Scheme 1.
(a) The photophysical process of TTA-UC. (b) The reported strategies for preparation TTA-UCNPs.

Table 1.

Summarized reported strategies for preparation of TTA-UCNPs

Nanoparticles	photosensitizer	emitter	Excitation /emission wavelength
Liposomeencapsulated TTAUCNPs [36]	PdTPBP	perylene	630 nm /473 nm
TTA-UC nanomicelles [40]	PtOEP	9,10 -Diphenylanthracene (DPA)	532 nm / 435 nm
TTA-UC nanomicelles [41]	PtP$_4$COONa	Amide bond and quaternary ammonium salt modified DPA derivative	532 nm / 440 nm
Silica-coated TTA-UCNPs [49]	PdOEP	DPA	532 nm/ 430 nm
Silica-coated TTA-UCNPs [51]	PdTPBP	Perylene / 9, 10-bis (phenylethynyl) anthracene	635 nm / 470, 505 nm
Polymer encapsulated TTA-UCNPs [61]	PdTPBP	9, 10-bis (phenylethynyl) anthracene	633 nm / 505 nm
Polymer (PIB/PEG) encapsulated TTA-UCNPs [64]	PdTPBP	2,5,8,11-tetra(tert - butyl)perylene	630 nm/ 486 nm
PLA-PEG coated TTA-UCNPs [65–66]	PdOEP	DPA	532 nm / 430 nm
Soybean oil nano-droplet [67]	PtTPBP	BDP-G/BDP-Y	635 nm / 517 nm, 528 nm
Silica coated oil nanodroplet [71]	BDP-F	PEA	650 nm / 432 nm
3D TTA-UC MOF [81]	PdTCPP (Pd Porphyrin derivative)	DPA	532 nm / 440 nm
1 D TTA-UC MOF [82]	Por (Pt Porphyrin derivative)	DPA	532 nm / 435 nm

Author Manuscript Author Manuscript Author Manuscript Author Manuscript